The Crystal Structures of the Room Temperature and the Low Temperature Phase of Dimethylammonium Trifluoromethanesulfonate

Pascal D. C. Dietzel[a], Robert Dinnebier[b], and Martin Jansen[b,*]

[a] Oslo/Norway, SINTEF Materials and Chemistry and University, Centre of Materials Science and Nanotechnology and Department of Chemistry

[b] Stuttgart/Germany, Max-Planck-Institut für Festkörperforschung

Abstract. Dimethylammonium trifluoromethanesulfonate **1** was synthesized by reaction of trifluoromethanesulfonic acid with an excess of dimethylamine. A temperature variable synchrotron measurement on the polycrystalline substance reveals that **1** passes through a phase transition below room temperature. The transition occurs in the temperature range of $282-285$ K on heating and $272-280$ K on cooling as determined by DSC. The room temperature phase crystallizes in space group $Cmca$ ($a = 11.031(6)$ Å, $b = 18.466(14)$ Å, $c = 8.173(9)$ Å, $V = 1665(2)$ Å^3, $Z = 8$) and the low temperature phase in space group $P\,2_1/c$ ($a = 8.8717(18)$ Å, $b = 8.0838(16)$ Å, $c = 10.968(2)$ Å, $\beta = 92.128(4)°$, $V = 786.0(3)$ Å^3, $Z = 4$). The structures of both phases were determined by single crystal X-ray diffraction, but refinement did not yield satisfactory residuals for the low temperature phase because of twinning of the crystal. It was, therefore, independently solved from the synchro-

tron powder diffraction data using rigid body models of the constituent ions and ab-initio direct space methods. Both, the CF$_3$ group and the SO$_3$ group of the triflate ion, are rotationally disordered around the S$-$C bond, in the room temperature phase. In the low temperature phase, the triflate ion is well localized. Like in the alkali metal triflates, the triflate ions are arranged in double layers with the hydrophobic trifluoromethyl groups and the sulfonate groups, respectively, pointing towards each other. The dimethylammonium ion is located closer to the sulfonate group with contacts indicating hydrogen bonding. The packing in both phases is of the topological CsCl structure type.

Keywords: Trifluoromethanesulfonate; Dimethylammonium; Trifluoromethyl group; Crystal structure; Disorder; Phase transitions

Introduction

The alkali metal trifluoromethanesulfonates (triflates) have been intensively studied recently. They warrant this attention by the aptitude of these compounds to behave as ion conductors which is due to the large number of rotational degress of freedom of the triflate ion and the resulting possibilities of cation movability within the crystal lattice. Accordingly, emphasis has been put on investigations of the crystal structures [1–6], the ionic conductivities [4, 5, 7], and discussion of the correlated mechanism of ion movement by solid state NMR techniques [8–12].

In this paper, we report the synthesis and crystal structure determination of dimethylammonium triflate. The dimethylammonium ion can be considered to be a larger homologue of an alkali metal. The aspherical shape of the dimethylammonium ion may result in a more interlocked type of packing than is achieved with the spherical alkali metal cations, which would inhibit the free movability of

the ions. In the related compound ammonium triflate [13, 14], in which the asphericity of the cation is less pronounced, four phase transitions occur in the range of $113-523$ K [15].

Experimental Section

Synthesis. Dimethylammonium trifluoromethansulfonate was synthesized by dropwise adding trifluoromethanesulfonic acid to dimethylamine ($\sim$10 mL) that was kept at 195 K under argon in one leg of an H-shaped apparatus which contained a glass filter sieve between the two legs of the vessel. When a precipitate started to form on addition of the acid, the solution was filtered into the other leg. The cooling was removed, whereupon the dimethylamine distilled off leaving behind the colorless dimethylammonium trifluoromethansulfonate. The purity of the product was checked by comparing the X-ray powder diffractogram with the calculated powder diffractogram of the room temperature phase.

Single crystal X-ray structure determination. Intensity data of crystals of C$_3$H$_8$F$_3$NO$_3$S **1** ($M = 195.16$ g mol^{-1}) was collected on a Bruker Smart Apex CCD X-ray diffractometer at 293 K and 100 K. The data of the crystal at 293 K was processed with the SAINT software [16]. The structure was solved by direct methods using SIR2004 [17]. Full-matrix least-squares refinement against $|F|^2$ and localization of the remaining non-hydrogen atoms from difference fourier maps proceeded with the SHELXL-97 program [18]. All non-hydrogen atoms were refined with anisotropic thermal dis-

* Prof. Dr. Dr. h. c. Martin Jansen
Max-Planck-Institut für Festkörperforschung
Heisenbergstr. 1
D-70569 Stuttgart, Germany
Fax: +49-711-6891502
E-mail: m.jansen@fkf.mpg.de

Table 1 Selected crystallographic data for the single crystal structure determination of $[NH_2(CH_3)_2][CF_3SO_3]$ **1** at 293 and 100 K.

| T / K	293	100
space group	$Cmca$	$P2_1/c$
a / Å	11.031(6)	8.8717(18)
b / Å	18.466(14)	8.0838(16)
c / Å	8.173(9)	10.968(2)
β / °	90	92.128(4)
V / Å^3	1665(2)	786.0(3)
Z	8	4
d_{calcd} / g cm^{-3}	1.557	1.649
μ(Mo Kα) / mm^{-1}	0.405	0.429
2θ range /°	4.42-50.00	4.60-56.00
no. reflections measured	5689	10828
no. unique reflections	778 ($R_{int} = 0.1251$)	1876
no. observed reflections [a]	387	8688
no. parameters / restraints	94 / 0	103 / 0
R indices ($I > 2\sigma$)	$R_1 = 0.0510$	$R_1 = 0.1063$
	$wR_2 = 0.1001$	$wR_2 = 0.2857$
R indices (all data)	$R_1 = 0.0978$	$R_1 = 0.1195$
	$wR_2 = 0.1156$	$wR_2 = 0.2941$
GOF	0.882	1.198
max./min. peaks / e Å^{-3}	0.148/$-$0.181	1.708/$-$0.981

[a] Observation criterion: $I > 2\sigma(I)$.

placement parameters. The trifluoromethyl and the sulfonate group were found to be disordered. They were refined in two split positions related by a rotation of 180°. The ratio of the site occupation factors of these two possible orientations refined to ~2:1 for the CF_3 group and ~3:1 for the SO_3 group. Hydrogen atoms of the methyl groups were geometrically constructed at idealized positions and refined with isotropic thermal parameters proportional to the thermal parameter of the carbon atom to which they are attached. The sole crystallographically unique hydrogen atom at the nitrogen atom was localized from the difference fourier map. Its positional parameters and isotropic thermal parameter were freely refined.

The crystal at 100 K was found to be twinned with two components, and the data was accordingly integrated with SAINT utilizing two orientation matrices obtained with the help of the program GEMINI [19]. The structure was then solved by direct methods using SHELXS-97 [20] with an input file containing only the non-overlapping reflections of one component. Full-matrix least-squares refinement against $|F|^2$ was performed using a reflection file containing non-overlapping and overlapping reflections from both components and the hklf 5 option of SHELXL-97 [18]. The non-hydrogen atoms were refined anisotropically. Hydrogen atoms were assigned to idealized positions and refined with isotropic thermal parameters proportional to the thermal parameter of the atom to which they are attached.

Temperature variable synchrotron powder diffraction. In-situ X-ray powder diffraction data of dimethylammonium trifluoromethanesulfonate (DMA-triflate) at low temperature were collected in transmission geometry with a Cryostream 600 cold air blower (Oxford Cryosystems) on a motorized goniometer head at beamline X7B at the National Synchrotron Light Source (NSLS) at Brookhaven National Laboratory. X-rays of energy 13.5 keV were selected by a double flat crystal monochromator in ultra-high vacuum located 8 meters from the source. The size of the beam was adjusted to approximately 0.5 mm^2. As detector, a MAR 345 image plate reader was set up perpendicular to the beam path at a distance of approx. 165 mm from the sample. LaB$_6$ was used as an external standard to determine the beam center, sample-to-detector dis-
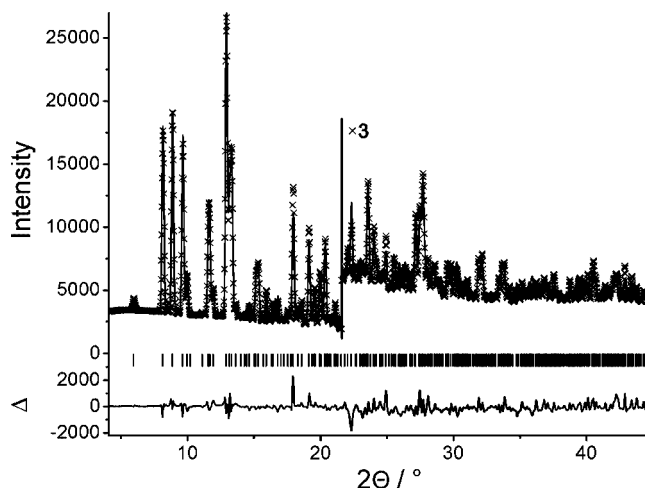
Figure 1 Rietveld refinement plots of dimethylammonium triflate **1** (crosses: observed pattern, line: calculated pattern, bottom line: difference plot. Bragg peaks are indicated by tick marks).

Table 2 Crystallographic data for the Rietveld refinement of the low-temperature phase of dimethylammonium trifluoromethane-sulfonate **1**.

formula	$C_3H_8F_3NO_3S$
formula weight / g mol^{-1}	106.1
T / K	137
space group	$P2_1/c$
Z	4
a / Å	8.8876(6)
b / Å	8.0619(9)
c / Å	10.9915(11)
β / °	92.556(6)
V / Å^3	786.77(18)
λ / Å	0.92234
2θ range /°	3.08-45.27
R_p	0.0334
R_{wp}	0.0475
R_{exp}	0.0231
$R(F^2)$	0.13116
no. of parameters	67
no. of restraints	47

tance, exact wavelength, and tilting angle of the image plate. The sample was contained in a sealed lithiumborate glass capillary with 0.5 mm diameter. The sample was aligned such that the sample was closest to the centre of the nozzle of the cold air blower at a distance of approx. 5 mm. The sample was cooled at a speed of 63 K/h from room temperature down to $T = 100$ K and reheated at a speed of 190 K/h back to room temperature. During exposure, the sample was spun in order to improve randomization of the crystallites. An exposure time of 240 seconds was chosen depending on the saturation intensity of the image plate. Together with a read-out time of 80 seconds of the image plate reader, this led to rates of 5.6 K/ scan for cooling and 16.9 K/ scan for heating. Integration of the full-circle powder patterns was performed using the program FIT2D [21, 22] resulting in diagrams of corrected intensities versus the scattering angle 2θ (figure 1). It was observed that the diffracted intensity was quite uniformly distributed over the Debye-Scherrer rings, ruling out severe grain size effects and preferred orientation. Low angle diffraction peaks had a typical FWHM of 0.18° 2θ. Further experimental details can be found in table 2.

Table 3 Relative atomic coordinates and isotropic displacement parameters (in Å^3) of the non-hydrogen atoms for the crystal structure determination of **1** at 293 K and 100 K.

Atom	Wyck.	x	y	z	U_{iso}
293 K					
S1	8f	0.0000	0.08658(7)	0.14210(15)	0.0834(6)
O1A	8f	0.0000	0.0956(3)	−0.0326(5)	0.122(3)
O2A	16g	−0.1066(5)	0.0603(2)	0.2004(9)	0.157(5)
O1B	8f	0.0000	0.0485(9)	0.299(2)	0.139(10)
O2B	16g	−0.1079(13)	0.0706(8)	0.063(2)	0.154(14)
C1	8f	0.0000	0.1787(3)	0.2120(9)	0.1107(18)
F1A	8f	0.0000	0.1826(4)	0.3717(9)	0.173(11)
F2A	16g	−0.0890(11)	0.2152(5)	0.1566(14)	0.173(7)
F1B	8f	0.0000	0.2169(19)	0.093(5)	0.36(4)
F2B	16g	−0.1040(19)	0.1940(8)	0.293(2)	0.179(18)
N1	8e	−0.2500	0.0626(3)	−0.2500	0.0983(14)
C2	16g	−0.3215(3)	0.1034(3)	−0.1369(4)	0.1284(16)
100 K single crystal solution					
S1	4e	0.17826(7)	0.34711(6)	0.53513(4)	0.01185(18)
O1	4e	0.1897(2)	0.5235(2)	0.51209(17)	0.0264(4)
O2	4e	0.1048(2)	0.2503(3)	0.44235(17)	0.0334(5)
O3	4e	0.1385(2)	0.3129(3)	0.65806(15)	0.0278(5)
C1	4e	0.3762(3)	0.2793(3)	0.5345(2)	0.0208(5)
F1	4e	0.3861(2)	0.1151(2)	0.55632(18)	0.0361(4)
F2	4e	0.4599(2)	0.3585(2)	0.61772(19)	0.0431(5)
F3	4e	0.4332(3)	0.3041(3)	0.42630(18)	0.0454(5)
N1	4e	0.1345(2)	0.7893(2)	0.23745(16)	0.0140(4)
C2	4e	0.2050(3)	0.6315(3)	0.1988(2)	0.0202(5)
C3	4e	0.2245(3)	0.8756(3)	0.3351(2)	0.0196(5)
100 K powder solution					
S1	4e	0.18048(50)	0.34491(60)	0.5350(5)	0.0111(16)
O1	4e	0.18079(130)	0.52087(100)	0.5086(11)	0.0111(16)
O2	4e	0.10217(110)	0.25293(130)	0.4403(10)	0.0111(16)
O3	4e	0.12927(110)	0.3103(13)	0.6546(8)	0.0111(16)
C1	4e	0.37903(70)	0.27429(90)	0.5377(7)	0.0461(33)
F1	4e	0.38531(100)	0.11737(110)	0.5649(10)	0.0461(33)
F2	4e	0.45728(110)	0.3584(13)	0.6202(10)	0.0461(33)
F3	4e	0.43561(100)	0.29657(130)	0.4311(8)	0.0461(33)
N1	4e	0.1402(12)	0.79327(170)	0.2321(13)	0.018(4)
C2	4e	0.2052(17)	0.6291(19)	0.2047(15)	0.018(4)
C3	4e	0.2157(5)	0.8689(16)	0.3408(12)	0.018(4)

Table 4 Anisotropic displacement parameters (in Å^2) for the single crystal structure determination of **1** at 293 K and 100 K.

Atom	U_{11}	U_{22}	U_{33}	U_{23}	U_{13}	U_{12}
293 K						
S1	0.1089(12)	0.0663(7)	0.0749(8)	−0.0100(6)	0.000	0.000
C1	0.174(7)	0.071(4)	0.087(5)	0.005(3)	0.000	0.000
F1A	0.34(3)	0.108(5)	0.067(5)	−0.027(3)	0.000	0.000
F2A	0.236(11)	0.098(6)	0.185(11)	−0.011(5)	0.003(9)	0.067(5)
O1A	0.181(9)	0.119(4)	0.064(3)	−0.017(3)	0.000	0.000
O2A	0.164(7)	0.103(3)	0.203(9)	−0.045(4)	0.087(7)	−0.055(4)
F1B	0.82(12)	0.076(14)	0.18(2)	0.084(17)	0.000	0.000
F2B	0.241(18)	0.128(9)	0.17(4)	−0.055(16)	0.06(2)	0.033(10)
O1B	0.21(3)	0.093(11)	0.110(13)	0.018(9)	0.000	0.000
O2B	0.128(12)	0.165(13)	0.17(2)	−0.097(14)	−0.109(16)	0.073(11)
N1	0.103(4)	0.080(3)	0.111(3)	0.000	0.024(3)	0.000
C2	0.112(3)	0.174(4)	0.099(3)	−0.039(3)	−0.003(2)	0.019(3)
100 K						
F1	0.0222(9)	0.0162(8)	0.0697(12)	0.0084(7)	−0.0015(8)	0.0047(7)
S1	0.0146(3)	0.0111(3)	0.0099(3)	−0.00165(17)	0.00072(19)	0.0022(2)
O1	0.0287(11)	0.0145(8)	0.0363(10)	0.0043(7)	0.0069(8)	0.0060(8)
O2	0.0286(11)	0.0376(11)	0.0330(10)	−0.0244(9)	−0.0136(8)	0.0153(10)
O3	0.0278(12)	0.0437(12)	0.0125(8)	0.0059(7)	0.0078(7)	0.0056(9)
C1	0.0185(12)	0.0135(11)	0.0306(12)	0.0030(9)	0.0020(10)	0.0007(9)
F2	0.0175(10)	0.0403(12)	0.0704(13)	−0.0059(9)	−0.0136(9)	−0.0039(8)
F3	0.0385(12)	0.0457(11)	0.0544(11)	0.0115(9)	0.0327(9)	0.0142(9)
N1	0.0174(11)	0.0095(9)	0.0149(9)	0.0012(7)	−0.0017(7)	0.0003(7)
C2	0.0268(16)	0.0145(11)	0.0194(11)	−0.0053(8)	0.0019(9)	0.0051(10)
C3	0.0255(14)	0.0131(11)	0.0195(11)	−0.0028(8)	−0.0088(9)	−0.0012(9)

Data reduction on all powder diffraction patterns was performed using the Powder3D program [23]. For the structure determination of the low temperature phase of DMA-Triflate, the data set at $T =$ 139 K was selected. Indexing with ITO [24] led to the lattice parameters given in table 2. The number of formula units per unit cell could be determined from volume increments. The extinctions found in the powder pattern indicated $P2_1/c$ as the most probable space group, which could later be confirmed by Rietveld [25] refinements. The crystal structure was solved by global optimization in direct space using the DASH [26] structure solution package [27]. The measured powder pattern at room temperature was subjected to Pawley refinements [28] in all possible space groups in order to extract correlated integrated intensities from the pattern. Good fits to the data were obtained. An internal coordinate description of the $(SO_3CF_3)^-$ moiety was constructed using bond lengths, angles and torsion angles from lithium triflate [1]. The position and orientation of the divalent cation $NH_2(CH_3)_2^+$ as well as the position, orientation, and torsion of the $(SO_3CF_3)^-$ anion in the unit cell were postulated and the trial structure was subjected to a global optimization. The structure giving the best fit to the data in space group $P2_1/c$ was validated by Rietveld refinement of the fractional coordinates obtained at the end of the simulated annealing run using the GSAS [29] program. To stabilize the refinements of the $(SO_3CF_3)^-$ anion, 17 soft constraints for the bond lengths (C−S, C−F, S−O; N−H, N−C, C−H) and 30 soft constraints for the bond angles (S−C−F, C−S−O; C−N−H, H−N−N, H−C−N) were used. The peak profiles and precise lattice parameters were determined by LeBail-type fits [30] using the program GSAS. The background was modeled manually using GUFI [31]. The peak-profile was described by a pseudo-Voigt function [32]. Lattice parameters, and cell volume of $[NH_2(CH_3)_2][CF_3SO_3]$ as a function of temperature were determined by LeBail fits for all data sets using GSAS (figure 5).

Selected crystallographic data are summarized in table 1. CCDC 600194, 600195, and 602816 contain the supplementary crystallographic data for this paper. These data can be obtained free of charge via www.ccdc.cam.ac.uk/datarequest/cif, by emailing data_request@ccdc.cam.ac.uk, or by contacting The Cambridge Crystallographic Data Centre, 12, Union Road, Cambridge CB2 1EZ, UK; fax: +44 1223 336033.

Results and Discussion

Crystal structures

Trifluoromethyl groups are often found to be rotationally disordered in crystal structure solutions at room temperature [33]. In the case of the trifluoromethanesulfonate ion, the SO_3 groups can also rotate around the S−C axis, and there may even be a dynamic exchange of the CF_3 and SO_3 groups at sufficiently high temperatures [11, 12]. Thus, it should be advantageous for the structure determination to freeze the dynamic disorder by working at lower temperatures. However, a single crystal study of **1** at 100 K revealed that the sample was twinned which is strongly indicative that a phase transition occurred on cooling. Although the structure could still be solved, refinement resulted in unsatisfactory residual factors which are likely to be an artefact of the twin integration of the diffraction data. We then confirmed that **1** passes through a phase transition by per-
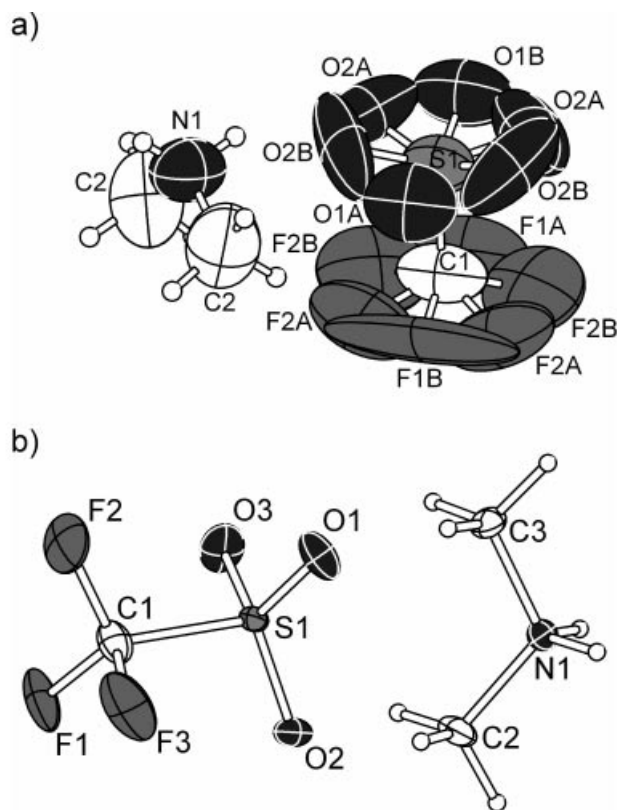
Figure 2 Molecular structure of dimethylammonium triflate **1** at 293 K (a) and 100 K (b) with atom-numbering scheme. Displacement ellipsoids are drawn at the 50 % probability level.

Table 5 Selected bond lengths /Å and angles /° for the single crystal structure determination of **1** at 293 K and 100 K.

293 K

S1−O2A	1.359 (4)	C1−F1B	1.20 (3)
S1−O2B	1.388 (10)	C1−F2A	1.274 (9)
S1−O1A	1.437 (5)	C1−F1A	1.307 (11)
S1−O1B	1.464 (17)	C1−F2B	1.354 (15)
S1−C1	1.794 (6)	N1−C2	1.430 (4)

100 K

F1−C1	1.351 (3)	C1−F2	1.321 (3)
S1−O2	1.4225 (19)	C1−F3	1.323 (3)
S1−O3	1.4333 (17)	N1−C3	1.485 (3)
S1−O1	1.4527 (19)	N1−C2	1.489 (3)
S1−C1	1.840 (3)		
O2−S1−O3	116.38 (14)	F2−C1−F1	108.8 (2)
O2−S1−O1	116.67 (13)	F3−C1−F1	106.5 (2)
O3−S1−O1	111.99 (12)	F2−C1−S1	111.42 (18)
O2−S1−C1	104.21 (12)	F3−C1−S1	110.82 (17)
O3−S1−C1	102.38 (12)	F1−C1−S1	110.39 (17)
O1−S1−C1	102.66 (12)	C3−N1−C2	112.80 (19)
F2−C1−F3	108.8 (2)		

Table 6 Hydrogen bonds in dimethylammonium triflate **1** at 293 K and 100 K.

D−H···A	d(D−H) / Å	d(H···A) / Å	d(D···A) / Å	∠(D−H···A) / °
293 K				
N1−H1···O2A	0.82(6)	2.10(7)	2.796(7)	142(6)
100 K				
N1−H1A···O1	0.92	2.09	2.955(3)	156
N1−H1B···O3	0.92	1.93	2.840(3)	169

forming a temperature variable synchrotron diffraction experiment on a powdered sample. To support the results of the single crystal structure determination, the crystal structure of the low temperature phase was independently solved from the synchrotron data using rigid body models of the constituent ions and ab-initio direct space methods. Both structure solutions, from single crystal data and from powder data, agree well with each other. The structure of the room temperature phase was determined from single crystal data. It was refined to satisfactory residuals even though the $I/\sigma(I)$ ratio falls below 2 for θ above ~19° which is a typical observation for compounds containing disorder. Selected crystallographic data for the single crystal structure determinations and the Rietveld refinement from synchrotron data are given in tables 1 and 2. Atomic coordinates and anisotropic displacement parameters are listed in tables 3 and 4. Table 5 contains selected geometric parameters.

Both, the trifluoromethyl as well as the sulfonate group, are rotationally disordered around the C−S bond in the room temperature phase, and the absolute magnitude of the displacement parameters of the dimethylammonium ion also indicates a certain degree of positional freedom for the cation (figure 2a). The shape of the anisotropic displacement parameter of C1 and the C−S bond length which is slightly shorter than in the low temperature structure may

mean that the triflate ion is additionally either subject to a dynamic oscillating motion with a small amplitude along [100] or a static displacement to both sides of the bc plane. In contrast, both ions are well localized at 100 K (figure 2b). The conformation of the triflate ion is staggered as is commonly found. The anions in both phases are arranged in the typical double layer fashion also found in the triflate of lithium, sodium, and cesium [1−3, 5, 6], in which the trifluoromethanesulfonate ions are arranged such that the fluoroorganic groups in adjacent layers face each other, and the hydrophilic sulfonate groups do likewise. The dimethylammonium ions are located exclusively close to the sulfonate groups (figure 3 center and right), and the hydrogen atoms of the nitrogen are involved in hydrogen bonds with oxygen atoms of the sulfonate group (table 6).

The space group *Cmca* of the room temperature phase is a minimal non-isomorphic supergroup of the monoclinic space group *P* $2_1/c$ of the low temperature phase. The unit cell of the orthorhombic unit cell at room temperature is related to the monoclinic one of the low temperature phase by $\boldsymbol{a} = \boldsymbol{c'}$, $\boldsymbol{b} = 2\boldsymbol{a'}$, and $\boldsymbol{c} = \boldsymbol{b'}$. In the room temperature phase, the dimethylammonium and the triflate ions are located on special positions. On passing through the phase
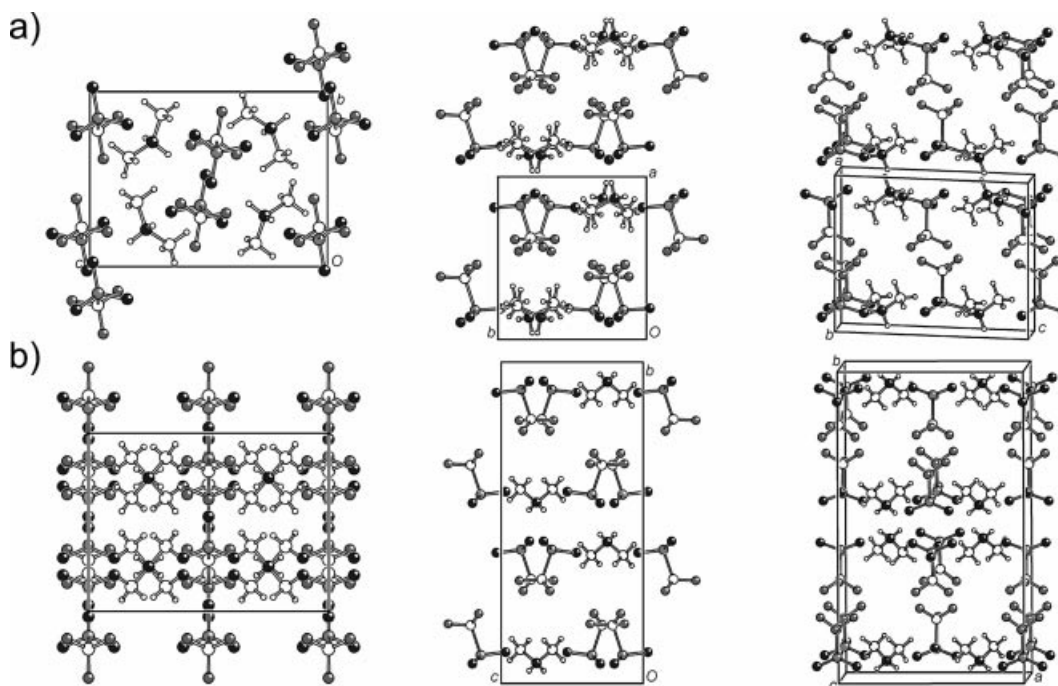
Figure 3 Comparison of the packing in the low temperature (a; view along *a*, *c*, and *b*, respectively, from left to right) and in the room temperature phase (b; view along *b*, *a*, and *c*, respectively, from left to right) of dimethylammonium triflate **1**. Only one orientation of the disordered EX₃ groups in the room temperature phase is shown for clarity. A second unit cell is drawn along the *a* axis for the low temperature phase to emphasize the relationship between the two structures.

transition, not only does the rotation of the EX_3 groups in the triflate cease, but they leave the special positions and alternatingly shift to both sides of the *ab* plane of the monoclinic phase (figure 3 left). The same occurs to the dimethylammonium ion in respect to the *ac* plane (figure 3 center). In addition, it is located on a glide plane in the orthorhombic phase, and each quadrant of the projection of the unit cell onto the *ac* plane contains the dimethylammonium ion in two orientations (figure 3b left). In the monoclinic phase, with the triflate ions being less uniformly positioned than in the orthorhombic phase, there is only one preferred orientation of the dimethylammonium ion per quadrant (now in the *bc* plane, figure 3a left).

The packing principle of both phases becomes apparent when the ions are replaced by their center of gravity (figure 4). Each center of gravity is surrounded by eight counterions within $4.32-5.77$ Å in the monoclinic phase and $4.53-5.76$ Å in the orthorhombic phase, respectively. The next closest anion-cation distance is more than 3 Å distant. The coordination polyhedron resembles a distorted cuboid. The packing is then topologically of the cesium chloride structure type.

Differential scanning calorimetry

The DSC measurements indicate three closely spaced thermal effects within a short temperature range (figure 5). On heating, there first occurs a less intense endothermic peak with a maximum between $281.7-282.7$ K, followed by a

significantly sharper and more intense endothermic peak at 285.35 K which actually has a shoulder at the slightly lower temperature of 284.6 K. (The peak positions shift slightly by ~0.4 K towards lower temperatures when the scan rate is reduced to 1 °C/min.) On cooling, a strong exothermic peak is observed with a maximum at 279.8 K. The shoulder is not clearly discernible, though the peak shape is not symmetric either. The maximum of the weaker exothermic peak that follows is located in the range of $272.5-274$ K. It is judicious to ascribe the intense signals to the crystallographic phase transition from the orthorhombic to the monoclinic phase and vice versa, but we can only surmise that the broader weak signal is caused by the onset or freezing in, respectively, of the rotation of the CF_3 and SO_3 groups. No further thermal effects are observed in the temperature range of 103 to 313 K. This includes the absence of further phase transitions. For comparison, ammonium triflate passes through three phase transitions in the same temperature interval [15].

Temperature variable synchrotron diffraction

The phase transition between the room temperature and the low temperature phase occurs in thermodiffraction pattern ~$20-30$ K below the temperature found in the DSC experiment (figure 6). On cooling, all three lattice parameters of the low temperature phase decrease with the temperature with the unit cell volume showing a linear dependency. The temperature range in which the room temperature phase
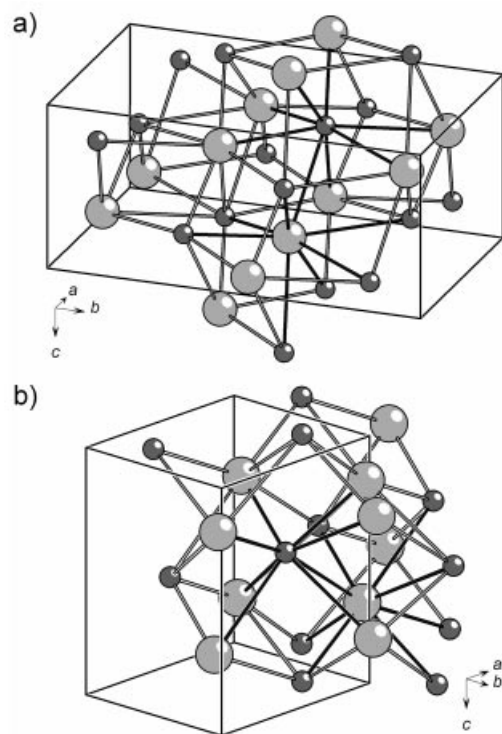
Figure 4 Topological representation of the packing in the room temperature (a) and low temperature (b) structure of dimethylammonium triflate **1** that illustrates the similarity to the cesium chloride structure type. The molecular ions are represented by their center of gravity (dimethylammonium: light grey, triflate: dark grey). One full set of short contacts around one cation and anion each is colored grey for emphasis.
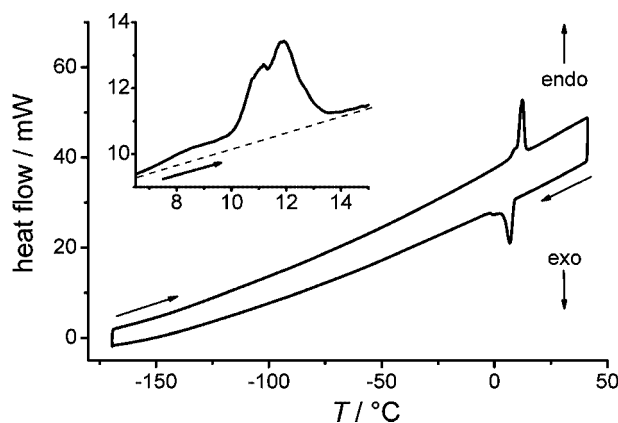

Figure 6 Powder diffraction patterns, lattice parameters, and cell volume of $NH_2(CH_3)_2[CF_3SO_3]$ as a function of temperature in the range from $T = 298$ K down to $T = 100$ K (65 K/h) and up to $T = 298$ K (190 K/h).

phase and, thus, it is largely responsible for the increase in volume.

Conclusion

Dimethylammonium triflate **1** is obtained in quantitative yield by reaction of trifluoromethanesulfonic acid with di-methylamine. It is found to pass through one structural phase transition in the investigated temperature range of 103 to 313 K. The number of phases is therefore substantially reduced in comparison with ammonium triflate. The less spherical dimethylammonium ion apparently facilitates a more optimal packing arrangement which reduces the number of degrees of motional freedom of both ions in the crystal packing. The trifluoromethanesulfonate ion is rotationally disordered around the S−C bond for both EX_3 groups in the orthorhombic room temperature phase. In the monoclinic low temperature phase, the motion is frozen. The crystal structure contains double layers of triflate ions, in which groups of similar polarity face each other, and the cations are located in the vicinity of the hydrophilic sulfonate group. The packing principle of both phases derives from the cesium chloride structure type.

Figure 5 DSC plot of dimethylammonium triflate **1** recorded with a scan rate of 5 °C/min (inset: 1 °C/min).

could be observed is too small to allow for an analysis of the lattice parameter trend. A discontinuous increase of the unit cell volume is observed when the phase transition occurs, which is in accordance with the additional space requirements of the rotating EX_3 groups. The *b* axis of the room temperature phase is significantly more than twice as large as the corresponding *a* axis of the low temperature
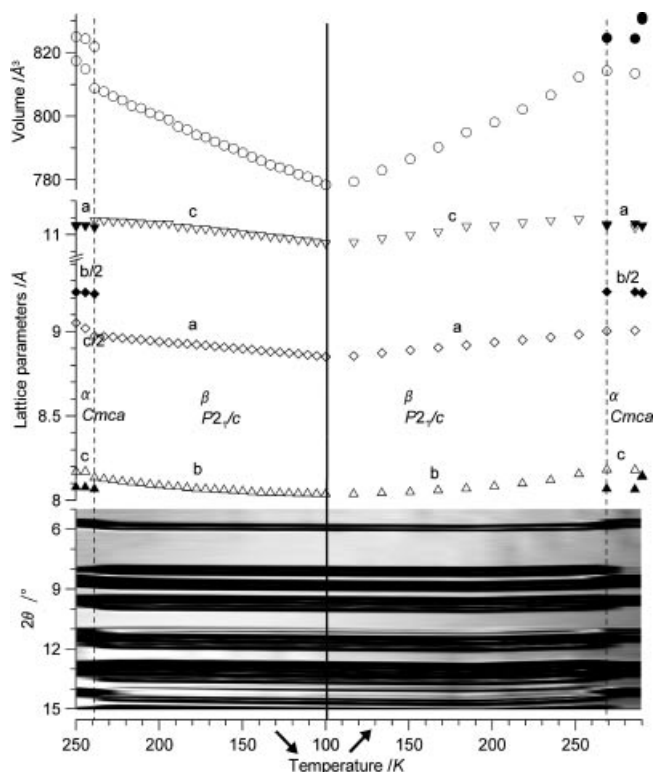
References

[1] M. Tremayne, P. Lightfoot, M. A. Mehta, P. G. Bruce, K. D. M. Harris, K. Shankland, C. J. Gilmore, G. Bricogne, *J. Solid State Chem.* **1992**, *100*, 191.

[2] M. Bolte, H. Lerner, *Acta Crystallogr.* **2001**, *E57*, m231.

[3] R. Dinnebier, N. Sofina, M. Jansen, *Z. Anorg. Allg. Chem.* **2004**, *630*, 1613.

[4] G. Korus, M. Jansen, *Z. Anorg. Allg. Chem.* **2001**, *627*, 1599.

[5] N. Sofina, E.-M. Peters, M. Jansen, *Z. Anorg. Allg. Chem.* **2003**, *629*, 1431.

[6] L. Hildebrandt, R. Dinnebier, M. Jansen, *Z. Anorg. Allg. Chem.* **2005**, *631*, 1660.

[7] M. Pompetzki, L. van Wüllen, M. Jansen, *Z. Anorg. Allg. Chem.* **2004**, *630*, 484.

[8] C. I. Rathcliffe, B. A. Dunell, *J. Chem. Soc., Faraday Trans.* **1981**, *77*, 2169.

[9] M. Mortimer, E. A. Moore, M. A. K. Williams, *J. Chem. Soc., Faraday Trans.* **1992**, *88*, 2393.

[10] M. Mortimer, E. A. Moore, M. A. K. Williams, *J. Chem. Soc., Faraday Trans.* **1996**, *92*, 5043.

[11] L. van Wüllen, N. Sofina, M. Jansen, *Chem. Phys. Chem.* **2004**, *5*, 1906.

[12] L. van Wüllen, L. Hildebrandt, M. Jansen, *Solid State Ionics* **2005**, *176*, 1449.

[13] F. A. Schröder, B. Gänswein, G. Brauer, *Z. Anorg. Allg. Chem.* **1972**, *391*, 295.

[14] B. Gänswein, G. Brauer, *Z. Anorg. Allg. Chem.* **1975**, *415*, 125.

[15] B. Gänswein, V. Kraemer, *Thermochim. Acta* **1976**, *16*, 395.

[16] SMART32 and SAINT32. Bruker AXS Inc., Madison, Wisconsin, USA, **2000**.

[17] M. C. Burla, R. Caliandro, M. Camalli, B. Carrozzini, G. L. Cascarano, L. De Caro, C. Giacovazzo, G. Polidori, R. Spagna, *J. Appl. Cryst.* **2005**, *38*, 381.

[18] G. M. Sheldrick, SHELXL97. Program for the Refinement of Crystal Structures (Release 97-2). Universität Göttingen, Germany, **1997**.

[19] GEMINI. Program for twinning solution. Bruker AXS Inc., Madison, Wisconsin, USA, **2000**.

[20] G. M. Sheldrick, SHELXS97. Program for the Solution of Crystal Structures (Release 97-2). Universität Göttingen, Germany, **1997**.

[21] A. P. Hammersley, *FIT2D*, Vers. 9.129, ESRF Internal Report ESRF98HA01T.

[22] A. P. Hammersley, S. O. Svenson, M. Hanfland, D. Hauserman, *High Pressare Res.* **1996**, *14*, 235.

[23] B. Hinrichsen, R. E. Dinnebier, M. Jansen, *Z. Krist. Suppl.* (EPDIC IX proceeding) **2006**, *23*, 231.

[24] J. W. Visser, *J. Appl. Crystallogr.* **1969**, *2*, 89.

[25] H. M. Rietveld, *J. Appl. Crystallogr.* **1969**, *2*, 65.

[26] DASH − Crystal Structure Solution from Powder Diffraction Data, Version 3.0. The Cambridge Crystallographic Data Centre, **2005**.

[27] W. I. F. David, K. Shankland, N. Shankland, *Chem. Commun.* **1998**, 931.

[28] G. S. Pawley, *J. Appl. Crystallogr.* **1981**, *14*, 357.

[29] A. C. Larson, R. B. von Dreele, *GSAS*, Vers. 2002, Los Alamos National Laboratory Report LAUR 86-748, Los Alamos, USA.

[30] A. Le Bail, H. Duroy, J. L. Fourquet, *Mater. Res. Bull.* **1988**, *23*, 447.

[31] R. E. Dinnebier, L. Finger, *Z. Krist.* **1998**, *Supplement Issue 15*, 148.

[32] P. Thompson, D. E. Cox, J. B. Hastings, *J. Appl. Crystallogr.* **1987**, *20*, 79.

[33] P. D. C. Dietzel, M. Jansen, *Z. Anorg. Allg. Chem.* **2004**, *630*, 1573.